Annals of R.S.C.B., ISSN:1583-6258, Vol. 25, Issue 4, 2021, Pages. 9758 - 9766
Received 05 March 2021; Accepted 01 April 2021.

Structured Analysis Sparsity Learning and Deep Learning for Image Restoration

[1]T.Jayachandran,[2]Dr.O.Cyril Mathew,[3]P.SenthilKumar, [4]Dr.K.Sharmilee

[1]Assistant profesor,Deparment of ECE, Nandha engineering college, Erode, India, Erode, India
[2]Assistant Professor, Department of ECEAl Ameen Engineering College, Erode, India
[3]Assistant Professor, Department of ECE,Velalar College of Engineering and Technology, Erode, India
[4]Assistant Professor, Department of ECE,Nandha Engineering College, Erode, India

Abstract**—**The restore of images states to a class of unknown reverse problems that recover unknown images. Image Previous is well known to be an important factor in designing solution algorithms to impose problems with image restore. The picture can be previously obtained through model-based or learning-based methods, depending on the accessibility of training data. In model-based approaches a mathematical construction of a penalty function is used to obtain a preliminary view and its parameters must be calculated within from the corrupted monitoring data. The picture before is used externally with the training data for learning-oriented approaches — for example, a deep convoluted neural network is training to study how to map the images from degraded to restored spaces. In the past decade we will review the important advances of each model that have inspired the creation of a hybrid (interior + external) that can be trained previously in this work. Experimental findings show that the projected techniques for SASL image restoration work in comparison with and often better than modern technology

Keywords—*Structured analysis sparsity learning, Image restoration, Deep learning and Sparse prior.*

I. Introduction

Initially, research on image restoration cantered on developing manual image models to solve reverse problems that involve a prior knowledge of natural image structure. To that end, a spectrum from linear differential operators with smooth signal compliance, to complete variation, [2] or wavelet sparsely [3] have been explored. Later, just over ten years ago, paradigms for image restoration moved to data-driven approaches. For example, a non-localized medium [4] is a non-parametrical estimator, which uses ground-breaking texture synthesis picture similarities[5]; numerous popular methods have focused on unsupervised learning such as sparse modelling[6], Gaussian mixture scales[7] or expert fields[8]. [4]. Modeled images combined, in particular, with auto similarities and scarce depictions, further enhance the consistency of the reconstruction of various restoration tasks [9]. The most popular approach is potentially blocked with 3D filtration (BM3D) [10].

Just recently, deep learning models have outperformed this last class of methods which are able to clean images for supervised training. More specifically, in various tasks, such as demonising [11-12], demo-seizures [13], super resolution [14] or removal of the object, deep models demonstrated great performance. More specifically. However, they also have inherent limits including lack of interpretability, and a large number of parameters are often needed, as can be prohibited in some applications. Improving all these things is one of our paper's main motivations. Our purpose is to build image restore algorithms that bridge the performance gap between interpretable earlier methods and efficient parameters and the new profound learning models.

II. Related works

The image restoration is to improve the image quality by reversing damaging effects such as noise and blur in a computational manner. A very comprehensive analysis is a key area in image processing and signal processing, and a host of methods are available, for instance [15] for a recent study. The active implementation of computer education and data-driven techniques has led to the renewed interest and development in image restoration in the last few years. In broad terms, new methods can be broken up into three modules: classical methodologies that do not use ML in a special way, generative techniques for probabilistic models of ungraded natural pictures and discrimination methods that truly attempt to learn directly from degraded to clean imagery. Contrary to classification strategies, two groups to be contingent on the obtainability of training data for the latter.

A. Classical Models

This methods class focuses on local statistics on photographs and tries to hold edges. For example: complete variation [16], bilateral filters [17], anisotropic model for diffusion[18] and the regression kernel (KR)[19]. Examples

Annals of R.S.C.B., ISSN:1583-6258, Vol. 25, Issue 4, 2021, Pages. 9758 - 9766
Received 05 March 2021; Accepted 01 April 2021.

include: More recent approaches take advantage of non-local image statistics with the vital comment that similar patches often appear in an image. The Non-local Medium (NLM) method [20], block-matching and 3D filtering (BM3D) [21], as well as non-local versions of sparse and lower-grade methods of representation [22-25] are representative work. Specifically, BM3D extends the initially introduced non-local similarity idea to NLM and combines it instead of simple pixel averaging via collaborative patch-filtration measures. The non-local sparse method, e.g. the simultaneous sparse coding (LSSC), explores the concept of patch similarity and enforces patches with identical coefficients in the transform fields. Applying low grade restriction for SVD of patch stacks, the WNNM method [26] filters related patches together. For compressive picture recovery sensing, a non-local, low rank limit is applied by NLR-CS [24]. The GSR method [25] models natural images in the area of group sparsity and simultaneously exploits the intrinsic local and non-local sparseness. The widely used MSE as a similarity metric is inactive in high-noise and distortion images while the efficient search of similar patches/pixels is necessary for these non-local methods [27]. More recent approaches employ perceptually motivated similarity measures for improved restorative consistency (such as structural similarity Index (SSIM) and gradient similarity deviations (GMSD) [28-29].

B. Generative Learning Models

This methodology class seeks to learn probability simulations of natural images that are not degraded. A simple but powerful subclass comprises models which approximate the sparse delivery of natural images in gradient, e.g. the restriction of p-norm ($0<p<1$) to images derivatives [30-31]. K-singular decomposition (CSVD) [32], convolutional sparse coding (CSC) [33-34], expert fields (FoE) [35] and perceptions of patch log probability (EPLL) [36] are more expressive generation models. While KSVD and CSC assume picture patches can be approached via a linear mixture of a couple of atoms from an overcrowded dictionary which is learned from the data, FoE learns a set of filter whose image responses are assumed to be sparse (i.e., the image convolution and the filter). EPLL designs picture patches via GMM, and applies this patch before the entire image via HQS [37] approach. The plug-and-play technique [38-39] is also closely linked to our approach. In these methods Gaussian denoiser are used to regularize the images, by division of optimization methods such as ADMM [40], to resolve general inverse problems. The fundamental variance between these approaches and our method is that they use established Gaussian denoiser generatively, while through discriminatory education we learn all parameters, thus finding a better balance between high quality and time performance. Generative models are agnostic in the task of image restore, i.e. transferable to a deterioration of the image, modular in nature, and combined with any probability and additional priors in the time of the test. The downside to this is that they are usually costly to solve and hinder apps, particularly on mobile platforms, in real time.

C. Discriminative Learning Models

The dataset CSE-CIC-IDS2018 comprises 15 450 706 rows, each of which consists of 10 files, with 80 functions per row. The file contents are listed as follows, [41] RTF field (RTF) [42], CSF fields [43], trainable non-linear reaction diffusion model [45-46] and its extensions [45-46] are representative examples. Using the FoEmodel[35], state-of-the-art CSF and TRD approaches can be derived by unrolling the corresponding optimisation iterations in feedback networks, in which each network's parameters are trained by lessening the error among its output images and the grounds truth for each mission. Neural imaging networks [47], deeper convolutional networks [48]–[50], deep recurrent neural networks [51] are often used as a research line. Discriminative methods must be based on a specific feedback structure with its computational efficiency during the course of training. These learned parameters will be held at test times and the calculation costs will be set. On the contrary, discriminatory models do not generalize tasks and generally require different feed architectures and a distinct training for each task (del-noising and de-nosing), as well as any image degradation necessary.

III. PROPOSED SYSTEM

In this work, we suggest the method of DTL that blends the strengths of generative and discrimination models, which retains the versatility of generative models while still achieving the computational efficiency of discriminatory models. In this work, we suggest the techniques of DTL. Figure 1, which expands the iterative steps of Algorithm 1 shows the key architecture for the proposed implementation of restoration network.

Annals of R.S.C.B., ISSN:1583-6258, Vol. 25, Issue 4, 2021, Pages. 9758 - 9766
Received 05 March 2021; Accepted 01 April 2021.

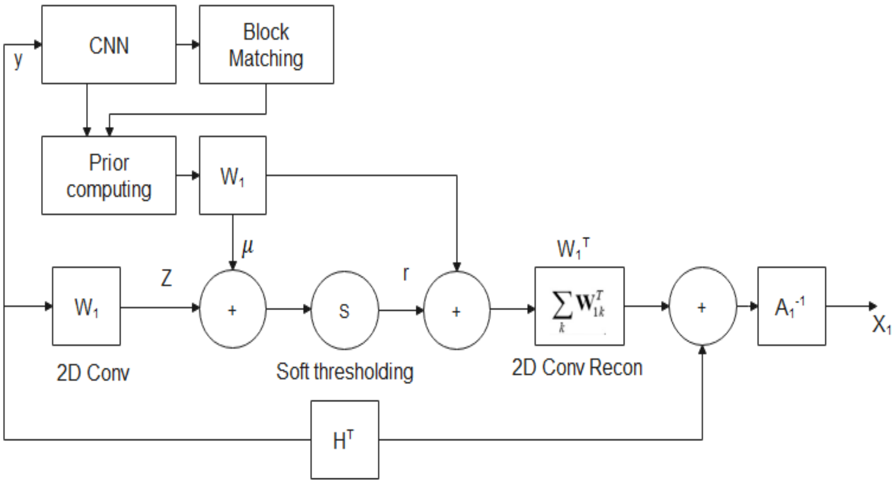

Fig.1. The proposed network for image restoration.

A. Prior pre-learning from training dataset

We aim to find out the function maps $z_k$of a needed restored frame x in regard to $W_k$filters for one particular picture of the observation y. The learning feature can be described as follows without losing generality

$$\hat{z} = G(y;\Theta)(1)$$

Where, $\hat{z} = [\hat{z}_1, \hat{z}_2, \ldots \hat{z}_k]$ and $G(\cdot)$ identifies the èas parameterized learning function. Because of the good abilities of CNN, we want to learn $z_k$on a profound CNN (DCNN). Any current DCNN can be used as a pre-learning phase to estimate x initially.

Similar to SRCNN [52] we have implemented the DCNN architecture. In contrast to Dong et al. [53], more convolution layers are used to increase estimation accuracy but less filter sizes are used. The CNN comprises 12 coil layers, each using K = 64 filters size 3 lines 3 lines 3 lines 64 lines. A single filter in size 3 to 3 is used to rebuild the last sheet. The input to output inspired by the deep residual learning provides a shortcut or skip relation (not exposed in the figure) (similar to Kim et al. [53]). DCNN training can be described as the objective feature

$$\Theta = \underset{\Theta}{argmin} \sum_i ||CNN(y_i;\Theta) - x_i||_2^2 \qquad (2)$$

Where, $y_i$and $x_i$indicate the image-pair observed and target trains and $CNN(y_i;\Theta)$ alternatively), the CNN output with Θ parameter is indicated. The back propagation algorithm optimizes all network parameters. The x calculation allows to estimate the set of feature maps through a set of analysis filters w_k i.e., $\hat{z}_k = w_k * \hat{x}, k = 1,2, \ldots, k$. Fig. 2 shows several examples of the studied turmoil filters w k..

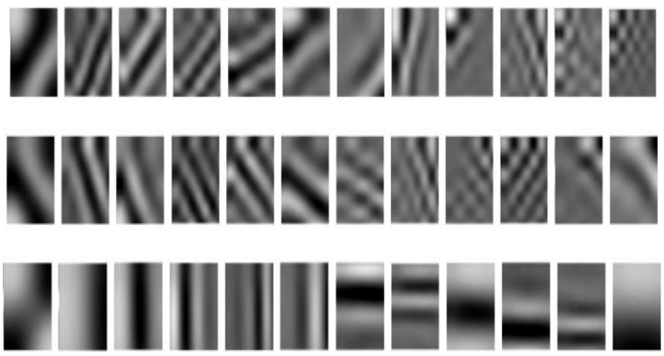

Fig.2. Visualization analysis filters in the first SASC phase.

Annals of R.S.C.B., ISSN:1583-6258, Vol. 25, Issue 4, 2021, Pages. 9758 - 9766
Received 05 March 2021; Accepted 01 April 2021.

B. Developing nonlocal self-similarity

We can also get the $z_k$projections from an internal estimation of the target image as well as externally learning the previous feature maps by way of CNN. In view of the fact that the natural images comprise rich repetitive patterns, the weighting of $z_{i,k}$over similar patches contained in the local window can be gained by means of the weighted mean of sparse codes (e.g., 20×20). Let $\hat{x}_{i_l}, l = 1, 2, \ldots, L$ indicate that the related patches in the L matches are nearest and $G_i = i_1, i_2 \ldots, i_L$indicate that the patches in the patchs are similar. Non-local $\hat{z}_{i,k}$estimates can be determined as

$$\tilde{z}_{i,k} = \sum_{l=1}^{L} w_{i_l} w_k^T \hat{x}_{i_l} = w_k^T \hat{x}_i (3)$$

Where, $w_{i_l} = \frac{1}{c}\exp(-\|\hat{x}_{i_l} - \hat{x}_i\|/h)$, $c$is a normalization constant, x I is a preset constant, and x \"sustainable I =support (l=1)^L" is a normalizing constant, $\tilde{x}_i = \sum_{l=1}^{L} w_{i_l}, \hat{x}_{i_l}$. is a constant, and x supposed"(s) is a continuous standardizing constant. The Eq. (3) It can be found that a non-local sparse code estimate can be obtained by first computing a followed non-local target image estimate.

By 2D filter convolution the w kill k. by 2D convolution. A stronger hybrid before feature maps can be obtained at Equation by comparing the estimate obtained with the non-local and CNN estimates. Eq.(4)

$$\mu_k = \delta \hat{z}_k + (1 - \delta)\tilde{z}_k (4)$$

Where, $0 < \delta < 1$is a constant selected. Algorithm 1 summarizes the Sparse Code (SASC) [54] overall organized research model for image recovery. In order to achieve a satisfactory result, Algorithm 1 usually requires thousands of iterations. The proposed SASC model is thus costly for measurement, while the algorithm 1 analyses filters are fixed. A deeper neural network is to approximate the proposed SASC model and, most significantly, the proposed structured analysis sparsity should be learned/trained from the source of the hybrid prior to the proposed model. We can optimize the parameters μm, μ and analysis filters for $w_k$together via end-to-end training, as next developed.

Algorithm 1 Image restoration with SASC
Initialization:
(a) Set parameters η and λ;
(b) Compute the initial estimate $\hat{x}^{(0)}$ by the CNN;
(c) Group a set of similar patches G_i for each patch $\hat{x}_i$using $\hat{x}^{(0)}$;
(c) Compute the prior feature maps μ_k using Eq. (14);
Outer loop: Iteration over t = 1, 2, . . . , T
(a) Compute the feature maps $z_k^{(t)}$, $k = 1, \ldots, K$ using [54]
(b) Update the HR image $\hat{x}^{(t)}$ via Eq. [54].
(c) Update μ_k via Eq. (14) based on $\hat{x}^{(t)}$;
Output: $x^{(t)}$.

IV. RESULTS AND DISCUSSION

Tensor Flow (training and testing) and MATLAB were used to implement the proposed algorithms. It takes about 49s to run SASC on an i7-5930k CPU machine (11.2s per iteration for an image of 256 to 256 as a result of our optimized implementation in MATLAB to find similar patches. Once the similar patches are found and saved, the real de-noise under Tensor Flow needs just 0,043s (i.e. the outcome of similar patches will be loaded directly); by comparison, DnCNN [55] takes around 1,44s to denoise the same picture on the same computer. We have extracted size 40 to 40 patches from the train400 data set [55] and used flip-and-rotation argumentation to produce 6000 to 128 patches in the training data. The most frequently used 12 pictures in [56] were the test collection (as shown in Fig. 3). Often used for benchmarking was the BSD 68 dataset. In that (a) is Man, (b) is House, (c) is Peppers, (d) is Starfish, (e) is Monar, (f) is Airpl, (g) is Parrot, (h) is Lena, (i) is Barbara, (j) is Boat and (k) is Man.(l) Coupl

Annals of R.S.C.B., ISSN:1583-6258, Vol. 25, Issue 4, 2021, Pages. 9758 - 9766
Received 05 March 2021; Accepted 01 April 2021.

e.

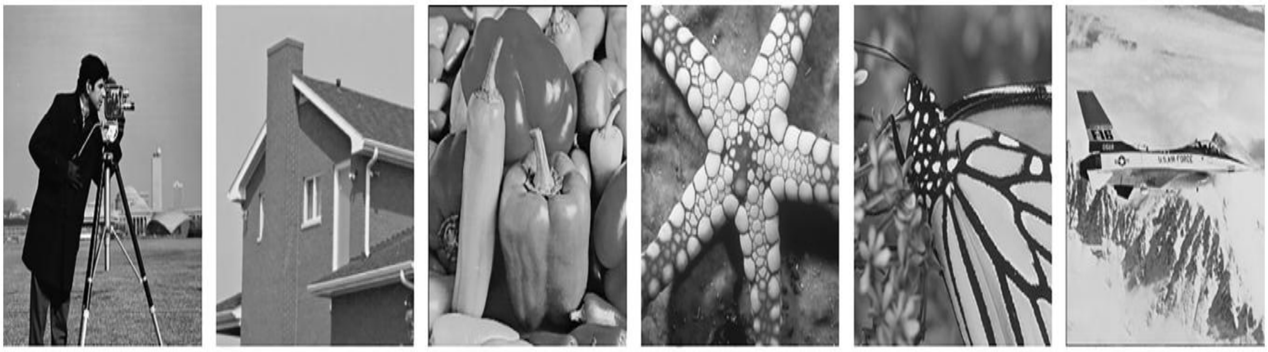

(a) (b) (c) (d) (e) (f)

(g) (h) (i) (j) (k) (l)

Fig. 3. The 12 test images used for image denoising.

We have applied numerous variants of the planned SASL network in proposed ablation study to provide an insight into the proposed network. The first variant is the scant coding (ASC) analytical network without CNN and prior self-similarity. We also current image restore results for use of the CNN only sub-network, which consists of twelve convolutionary layers that are non-linear with ReLU and three or three kernels (paragraph 3/64). SASL approach is the proposed full network of both CNN and previous learning.

TABLE I. AVERAGE SSIM/ PSNR OUTCOMES OF THE VARIANTS OF THE PROJECTED DENOISING TECHNIQUE.

		Set 12			BSD68		
		$\sigma = 15$	$\sigma = 25$	$\sigma = 50$	$\sigma = 15$	$\sigma = 25$	$\sigma = 50$
PSNR	ASC	32.61	30.32	27.12	31.67	29.14	26.03
SSIM		0.8923	0.8468	0.7511	0.8819	0.8089	0.6732
PSNR	CNN	32.89	30.29	27.14	31.76	29.36	26.34
SSIM		0.8879	0.8341	0.7601	0.8841	0.8112	0.6932
PSNR	proposed	33.73	30.99	27.98	32.16	29.93	27.19
SSIM		0.9032	0.8674	0.7913	0.8870	0.8289	0.7249

TABLE. II. AVERAGE PSNR/SSIM RESULTS OF THE ALTERNATIVES OF THE PROPOSED DEBLURRING METHOD.

		Set 12			BSD68		
		$\sigma = 2$	$\sigma = 2.55$	$\sigma = 7.65$	$\sigma = 2$	$\sigma = 2.55$	$\sigma = 7.65$
PSNR	ASC	33.40	32.40	28.70	32.96	32.29	28.43
SSIM		0.9203	0.9107	0.8417	0.9432	0.9105	0.8398
PSNR	CNN	33.22	32.72	28.87	33.13	32.64	28.54
SSIM		0.9765	0.9163	0.8576	0.9222	0.9854	0.8539
PSNR	proposed	34.05	33.17	29.16	33.94	32.95	28.74

Annals of R.S.C.B., ISSN:1583-6258, Vol. 25, Issue 4, 2021, Pages. 9758 - 9766
Received 05 March 2021; Accepted 01 April 2021.

SSIM		0.9255	0.9156	0.8580	0.9234	0.9136	0.8568

TABLE III. PSNR/SSIM RESULTS OF CHALLENGING DENOISING APPROACHES ON SET12 DATASET.

Image	monar	Airpl	C.man	house	peppers	starfish	parrot	Lena	Barb.	boat	man	coup	Avg
σ = 15													
BM3D[15]	31.86	31.08	31.92	34.94	32.70	31.15	31.38	34.27	33.11	32.14	31.93	32.11	32.38
EPLL [61]	31.03	31.16	31.82	34.14	32.58	31.08	31.40	33.87	31.34	31.91	31.97	31.90	32.10
TNRD [51]	32.57	31.47	32.19	34.55	33.03	31.76	31.63	34.25	32.14	32.15	32.24	32.11	32.51
DnCNN-s[59	33.10	31.70	32.62	35.00	33.29	32.23	31.84	34.63	32.65	32.42	32.47	32.47	32.87
WNNM[62]	32.72	31.40	32.18	35.15	32.97	31.83	31.61	34.38	33.61	32.28	32.12	32.18	32.70
Our proposed	33.30	31.98	32.16	35.55	33.29	32.23	32.21	35.19	33.93	32.99	32.93	33.08	33.31

The SASC approach outperforms the original ASC method in Table 1.The proposed SASL method further enhances the denoising efficiency by combining both external and internal precursors. Similar observation can be made between the proposed deblurringtechnique in Table 2 on two separate blur kernels.

The proposed technique has been compared with several common denotation methods, including three methods of model demoisation (BM3D)[57], EPLL[58], WNNM[59]) and two methods for deep learning (TNRD [60] and DnCNN-S [61]). Tables 3 illustrate comparative PSNR findings on grayscale picture data collection of competitive methods (Set12). The suggested approach can be shown to be much more effective than other competing methods. In particular, the planned method exceeds DnCNN-S [61] by 0.56 dB on average for the previous state-of-the-art method.

V. Conclusion

In this paper we are proposing to create a network of well-established, SASL models for image restoration. The proposed scheme is comparable to the current state-of-the-art restoration method and often even better. Trainable SASL also showed good widespread properties. The extension of existing works to blind imagery is a natural follow-up work. Restore degraded images of the real world including blurred kernels and unknown noise. For blind image denoise, comparisons with current trends on common benchmark datasets are very important; for blind image deblurring, SASL and the recent work on a blurred kernel estimate can be combined with an advantageous maximum local gradient. Comparison-oriented class learning recently developed can propose new ways to assess these blind image restore methods.

VI. Reference

[1]. P. Perona and J. Malik. Scale-space and edge detection using anisotropic diffusion. IEEE Transactions on Pattern Analysis and Machine Intelligence (PAMI), 12(7):629–639, 1990.
[2]. L. I. Rudin, S. Osher, and E. Fatemi. Nonlinear total variation based noise removal algorithms. Physica D: nonlinear phenomena, 60(1-4):259–268, 1992.
[3]. S. Mallat. A Wavelet Tour of Signal Processing, Second Edition. Academic Press, New York, 1999.
[4]. A. Buades, B. Coll, and J.-M. Morel. A non-local algorithm for image denoising. In Proc. Conference on Computer Vision and Pattern Recognition (CVPR), 2005.

Annals of R.S.C.B., ISSN:1583-6258, Vol. 25, Issue 4, 2021, Pages. 9758 - 9766
Received 05 March 2021; Accepted 01 April 2021.

[5]. A. Efros and T. Leung. Texture synthesis by non-parametric sampling. In Proc. International Conference on Computer Vision (ICCV), 1999.
[6]. J. Mairal, F. Bach, J. Ponce, et al. Sparse modeling for image and vision processing. Foundations and Trends in Computer Graphics and Vision, 8(2-3):85–283, 2014.
[7]. J. Portilla, V. Strela, M. Wainwright, and E. Simoncelli. Image denoising using scale mixtures of Gaussians in the wavelet domain. IEEE Transactions on Image Processing, 12(11):1338–1351, 2003.
[8]. S. Roth and M. J. Black. Fields of experts: A framework for learning image priors. In Proc. Conference on Computer Vision and Pattern Recognition (CVPR), 2005.
[9]. S. Gu, L. Zhang, W. Zuo, and X. Feng. Weighted nuclear norm minimization with application to image denoising. In Proc. Conference on Computer Vision and Pattern Recognition (CVPR), 2014.
[10].K. Dabov, A. Foi, V. Katkovnik, and K. Egiazarian. Image denoising by sparse 3-d transform-domain collaborative filtering. IEEE Transactions on image processing, 16(8):2080–2095, 2007.
[11].K. Zhang, W. Zuo, Y. Chen, D. Meng, and L. Zhang. Beyond a gaussiandenoiser: Residual learning of deep cnn for image denoising. IEEE Transactions on Image Processing, 26(7):3142–3155, 2017.
[12].T. Plötz and S. Roth. Neural nearest neighbors networks. In Proc. Advances in Neural Information Processing Systems (NIPS), 2018.
[13].Y. Zhang, K. Li, K. Li, B. Zhong, and Y. Fu. Residual non-local attention networks for image restoration. In Proc. International Conference on Learning Representations (ICLR), 2019.
[14].J. Kim, J. Kwon Lee, and K. Mu Lee. Accurate image super-resolution using very deep convolutional networks. 2016.
[15].P. Milanfar, "A tour of modern image filtering: New insights and methods, both practical and theoretical," IEEE Signal Process. Mag., vol. 30, no. 1, pp. 106–128, Jan. 2013.
[16].L. I. Rudin, S. Osher, and E. Fatemi, "Nonlinear total variation based noise removal algorithms," Phys. D, Nonlinear Phenomena, vol. 60, nos. 1–4, pp. 259–268, 1992.
[17].C. Tomasi and R. Manduchi, "Bilateral filtering for gray and color images," in Proc. IEEE Int. Conf. Comput. Vis. (ICCV), Jan. 1998, pp. 839–846.
[18].J. Weickert, Anisotropic Diffusion in Image Processing. Stuttgart, Germany: Teubner-Verlag, 1998.
[19].H. Takeda, S. Farsiu, and P. Milanfar, "Kernel regression for image processing and reconstruction," IEEE Trans. Image Process., vol. 16, no. 2, pp. 349–366, Feb. 2007.
[20].A. Buades, B. Coll, and J.-M. Morel, "A review of image denoising algorithms, with a new one," Multiscale Model. Simul., vol. 4, no. 2, pp. 490–530, 2005.
[21].K. Dabov, A. Foi, V. Katkovnik, and K. Egiazarian, "Image denoising by sparse 3-D transform-domain collaborative filtering," IEEE Trans. Image Process., vol. 16, no. 8, pp. 2080–2095, Aug. 2007.
[22].J. Mairal, F. Bach, J. Ponce, G. Sapiro, and A. Zisserman, "Non-local sparse models for image restoration," in Proc. IEEE Int. Conf. Comput. Vis. (ICCV), Sep./Oct. 2009, pp. 2272–2279.
[23].H. Talebi and P. Milanfar, "Global image denoising," IEEE Trans. Image Process., vol. 23, no. 2, pp. 755–768, Feb. 2014.
[24].W. Dong, G. Shi, X. Li, Y. Ma, and F. Huang, "Compressive sensing via nonlocal low-rank regularization," IEEE Trans. Image Process., vol. 23, no. 8, pp. 3618–3632, Aug. 2014.
[25].J. Zhang, D. Zhao, and W. Gao, "Group-based sparse representation for image restoration," IEEE Trans. Image Process., vol. 23, no. 8, pp. 3336–3351, Aug. 2014.
[26].S. Gu, L. Zhang, W. Zuo, and X. Feng, "Weighted nuclear norm minimization with application to image denoising," in Proc. IEEE Conf. Comput. Vis. Pattern Recognit. (CVPR), Jun. 2014, pp. 2862–2869.
[27].Z. Wang and A. C. Bovik, "Mean squared error: Love it or leave it? A new look at signal fidelity measures," IEEE Signal Process. Mag., vol. 26, no. 1, pp. 98–117, Jan. 2009.

[28].A. Rehman and Z. Wang, "SSIM-based non-local means image denoising," in Proc. IEEE Int. Conf. Image Process. (ICIP), Sep. 2011, pp. 217–220.
[29].V. Jakhetiya, W. Lin, S. P. Jaiswal, S. C. Guntuku, and O. C. Au, "Maximum a posterior and perceptually motivated reconstruction algorithm: A generic framework," IEEE Trans. Multimedia, vol. 19, no. 1, pp. 93–106, Jan. 2017.
[30].A. Levin, R. Fergus, F. Durand, and W. T. Freeman, "Image and depth from a conventional camera with a coded aperture," ACM Trans. Graph., vol. 26, no. 3, p. 70, 2007.
[31].D. Krishnan, T. Tay, and R. Fergus, "Blind deconvolution using a normalized sparsity measure," in Proc. IEEE Conf. Comput. Vis. Pattern Recognit. (CVPR), Jun. 2011, pp. 233–240.
[32].M. Elad and M. Aharon, "Image denoising via sparse and redundant representations over learned dictionaries," IEEE Trans. Image Process., vol. 15, no. 12, pp. 3736–3745, Dec. 2006.
[33].B. Wohlberg, "Efficient convolutional sparse coding," in Proc. IEEE Int. Conf. Acoust., Speech Signal Process. (ICASSP), May 2014, pp. 7173–7177.
[34].F. Heide, W. Heidrich, and G. Wetzstein, "Fast and flexible convolutional sparse coding," in Proc. IEEE Conf. Comput. Vis. Pattern Recognit. (CVPR), Jun. 2015, pp. 5135–5143.
[35].S. Roth and M. J. Black, "Fields of experts," Int. J. Comput. Vis., vol. 82, no. 2, pp. 205–229, Apr. 2009.
[36].D. Zoran and Y. Weiss, "From learning models of natural image patches to whole image restoration," in Proc. IEEE Int. Conf. Comput. Vis. (ICCV), Nov. 2011, pp. 479–486.
[37].D. Geman and C. Yang, "Nonlinear image recovery with half-quadratic regularization," IEEE Trans. Signal Process., vol. 4, no. 7, pp. 932–946, Jul. 1995.
[38].Y. Romano, M. Elad, and P. Milanfar. (Nov. 2016). "The little engine that could: Regularization by denoising (RED)." [Online]. Available: https://arxiv.org/abs/1611.02862
[39].S. A. Bigdeli, M. Zwicker, P. Favaro, and M. Jin, "Deep meanshift priors for image restoration," in Proc. Conf. Neural Inf. Process. Syst. (NIPS), 2017, pp. 763–772.
[40].S. Boyd, N. Parikh, E. Chu, B. Peleato, and J. Eckstein, "Distributed optimization and statistical learning via the alternating direction method of multipliers," Found. Trends Mach. Learn., vol. 3, no. 1, pp. 1–122, Jan. 2011.
[41].J. Sun and M. F. Tappen, "Separable Markov random field model and its applications in low level vision," IEEE Trans. Image Process., vol. 22, no. 1, pp. 402–407, Jan. 2013.
[42].J. Jancsary, S. Nowozin, T. Sharp, and C. Rother, "Regression tree fields—An efficient, non-parametric approach to image labeling problems," in Proc. IEEE Conf. Comput. Vis. Pattern Recognit. (CVPR), Jun. 2012, pp. 2376–2383.
[43].U. Schmidt and S. Roth, "Shrinkage fields for effective image restoration," in Proc. IEEE Conf. Comput. Vis. Pattern Recognit. (CVPR), Jun. 2014, pp. 2774–2781.
[44].Y. Chen, W. Yu, and T. Pock, "On learning optimized reaction diffusion processes for effective image restoration," in Proc. IEEE Conf. Comput. Vis. Pattern Recognit. (CVPR), Jun. 2015, pp. 5261–5269.
[45].L. Xiao, J. Wang, W. Heidrich, and M. Hirsch, "Learning high-order filters for efficient blind deconvolution of document photographs," in Proc. Eur. Conf. Comput. Vis. (ECCV), 2016, pp. 734–749.
[46].T. Klatzer, K. Hammernik, P. Knobelreiter, and T. Pock, "Learning joint demosaicing and denoising based on sequential energy minimization," in Proc. IEEE Int. Conf. Comput. Photogr. (ICCP), May 2016, pp. 1–11.
[47].H. C. Burger, C. J. Schuler, and S. Harmeling, "Image denoising: Can plain neural networks compete with BM3D?" in Proc. IEEE Conf. Comput. Vis. Pattern Recognit. (CVPR), Jun. 2012, pp. 2392–2399.
[48].V. Jain and H. Seung, "Natural image denoising with convolutional networks," in Proc. Conf. Neural Inf. Process. Syst. (NIPS), vol. 21. 2009, pp. 769–776.
[49].L. Xu, J. S. J. Ren, C. Liu, and J. Jia, "Deep convolutional neural network for image deconvolution," in Proc. Conf. Neural Inf. Process. Syst. (NIPS), 2014, pp. 1790–1798.

[50].M. Gharbi, G. Chaurasia, S. Paris, and F. Durand, “Deep joint demosaicking and denoising,” ACM Trans. Graph., vol. 35, no. 6, p. 191, 2016.

[51].S. Wang, S. Fidler, and R. Urtasun, “Proximal deep structured models,” in Proc. Conf. Neural Inf. Process. Syst. (NIPS), 2016, pp. 865–873.

[52].C. Dong, C.C. Loy, K. He, X. Tang, Image super-resolution using deep convolutional networks, IEEE Trans. Pattern Anal. Mach.Intell. 38 (2) (2016) 295–307.

[53].J. Kim, J. Kwon Lee, K. Mu Lee, Deeply-recursive convolutional network for image super-resolution, in: Proceedings of the IEEE Conference on Computer Vision and Pattern Recognition, 2016, pp. 1637–1645.

[54].Dong, Weisheng, Guangming Shi, Yi Ma, and Xin Li. "Image restoration via simultaneous sparse coding: Where structured sparsity meets gaussian scale mixture." International Journal of Computer Vision 114, no. 2 (2015): 217-232.

[55].K. Zhang, W. Zuo, Y. Chen, D. Meng, L. Zhang, Beyond a gaussiandenoiser: Residual learning of deep CNN for image denoising, IEEE Trans. Image Process. 26 (7) (2017) 3142–3155.

[56].K. Dabov, A. Foi, V. Katkovnik, K. Egiazarian, Image denoising by sparse 3-d transform-domain collaborative filtering, IEEE Trans. Image Process. 16 (8) (2007) 2080–2095.

[57].K. Dabov, A. Foi, V. Katkovnik, K. Egiazarian, Image denoising by sparse 3-d transform-domain collaborative filtering, IEEE Trans. Image Process. 16 (8) (2007) 2080–2095.

[58].S. Gu, L. Zhang, W. Zuo, X. Feng, Weighted nuclear norm minimization with application to image denoising, in: Proc. of the IEEE CVPR, 2014, pp. 2862–2869.

[59]. D. Zoran, Y. Weiss, From learning models of natural image patches to whole image restoration, in: Proc. of the IEEE ICCV, 2011, pp. 479–486.

[60].Y. Chen, T. Pock, Trainable nonlinear reaction diffusion: a flexible framework for fast and effective image restoration, IEEE Trans. Pattern Anal. Mach.Intell. 39 (6) (2017) 1256–1272.

[61].K. Zhang, W. Zuo, Y. Chen, D. Meng, L. Zhang, Beyond a gaussiandenoiser: Residual learning of deep CNN for image denoising, IEEE Trans. Image Process. 26 (7) (2017) 3142–3155.